



**Zn²⁺ ion of the snake venom metalloproteinase (SVMP)
plays a critical role in the ligand binding: A molecular
dynamics simulation study**

Journal:	<i>RSC Advances</i>
Manuscript ID:	RA-ART-07-2015-014693
Article Type:	Paper
Date Submitted by the Author:	24-Jul-2015
Complete List of Authors:	Muthusamy, Karthikeyan; Alagappa University, Department of Bioinformatics Chinnasamy, Sathishkumar; Alagappa University, Bioinformatics Nagamani, Selvaraman; Alagappa University, Bioinformatics

1 **Zn²⁺ ion of the snake venom metalloproteinase (SVMP) plays a critical role in the ligand**
2 **binding: A molecular dynamics simulation study**

3 Sathishkumar Chinnasamy, Selvaraman Nagamani and Karthikeyan Muthusamy*

4 Department of Bioinformatics, Alagappa University, Karaikudi-630 004, Tamil Nadu, India.

5

6

7

8

9

10

11

12

13

14 ****Corresponding author:***

15 Dr. Karthikeyan Muthusamy

16 Assistant Professor

17 Phone (Off): +91-4565-223344

18 Fax (Off): +91-4565-225202

19 Email: mkbioinformatics@gmail.com

1 Abstract

2 Snake venom metalloproteinase (SVMP) is one of the major components of snake venom
3 and it is a root causative agent for edema, local tissue damage, inflammation, blood coagulation
4 and hemorrhage during the snakebite. The catalytic activity of SVMP is regulated by the metal
5 ions (Zn^{2+} and Ca^{2+}). In this study, three dimensional structure of SVMP was modeled with Zn^{2+}
6 and Ca^{2+} ions. Molecular docking, Prime/MM-GBSA (ΔG_{bind} calculations), Quantum polarized
7 ligand docking (QPLD), QM-MM interaction energy analysis and molecular dynamics
8 simulation were performed for the compound *clerodane diterpenoid* with the SVMP in the
9 presence and absence of metal ions (Zn^{2+} and Ca^{2+}). The result shows that, the metal ions that are
10 present in ligand binding domain are critical for function of the SVMP protein, particularly the
11 Zn^{2+} ion. Further, we observed that both the ions have significant effect on ligand binding.

12 **Key words:** SVMP, Molecular Docking, MD simulation, QM-MM interaction energy
13 calculation.

14

15

16

17

18

19

20

1 Introduction

2 Snake venom is a complex mixture of proteins, peptides, inorganic compounds and metal
3 ions.^{1,2} Generally snakes use the venom for offensive weapons for immobilizing, killing and
4 digesting their prey.³ Approximately 20 different types of toxic enzymes were involved in snake
5 venom.⁴ The snake venom metalloproteinase (SVMP) has significant roles in the envenomation
6 pathogenesis, such as edema, inflammation, vascular clotting, hemorrhage and necrosis.⁵ The
7 SVMP is largely responsible for the hemorrhagic syndrome in snake envenomation^{6,7}; it is one of
8 the most serious consequences of snakebite.⁸ The SVMP is regulated by different mechanisms
9 such as, disruption of hemostasis mediated pro- or anti-coagulant effects (prothrombin,
10 activating activities, fibrinogenase, and fibrolase), apoptotic or pro-inflammatory activates and
11 platelet aggregation inhibitors.⁹⁻¹² The zinc dependent SVMP causes the hemorrhagic effects,
12 myonecrosis, skin damage, edema, and other associated inflammations as well as relevant
13 homeostatic and hematological alterations.¹³⁻¹⁵ In addition, the zinc dependent SVMP induced
14 hemorrhagic effect and directly affects the integrity of micro-vessel particularly capillaries.⁸ The
15 hemostatic and micro-vessel disturbances act synergistically to provoke profuse bleeding in
16 snake envenomation.^{16,17} The hemorrhagic toxins independently induce bleeding in absence of
17 hemostatic alterations.⁸ Thus, some of these SVMP have applications for treating human
18 conditions involving abnormal blood clotting.^{18,19} The SVMP also involved in additional
19 mechanism of hemorrhage, it can be caused by base membrane and disturbing the interactions
20 between endothelial cells through the degradation of endothelial cell membrane proteins (e.g.,
21 integrin, cadherin) and basement membrane components (e.g., fibronectin, laminin, nidogen,
22 type IV collagen).²⁰

1 The *clerodane diterpenoid* was significantly inhibited by hemorrhagic activity. The total
2 inhibition of hemorrhagic activity suggested interaction of *clerodane diterpenoid* with metal/or
3 metalloproteases, neutralizing effects. It is much more efficient to inhibit the pharmacological
4 activities induced by metalloproteinase. This inhibitor was able to neutralize the
5 fibrinogenolytic and caseinolytic activities of snake venom metalloproteinase. The *clerodane*
6 *diterpenoid* inhibitor shows that a strong O-H...O hydrogen bond. This intermolecular
7 interaction is between atoms O3-H3... O1 and it is responsible for the formation of an infinite
8 chain along the a-axis.

9 In this study, the zinc dependent SVMP (*Echis coloratus* (Carpet viper)) modeled
10 protein²¹ was used for the analysis. The molecular docking study was performed for the molecule
11 *clerodane diterpenoid* (a potent SVMP inhibitor) with SVMP in the presence and absence of
12 metals (Zn^{2+} and Ca^{2+}). Prime/MM-GBSA (ΔG_{Bind} calculations and Quantum polarized ligand
13 docking (QPLD) analyses were also performed for SVMP in the presence and absence of metals
14 (Zn^{2+} and Ca^{2+}). Furthermore, the docking studies were supported by QM-MM interaction
15 energy analysis. Further the stability of the protein ligand complexes were performed by MD
16 simulation using Desmond.

17 **Materials and methods**

18 **Protein preparation**

19 The SVMP modeled protein was prepared using protein preparation wizard of Glide
20 software (Schrödinger, LLC, New York, NY, 2014) (presence of both Zn^{2+} and Ca^{2+} ions
21 (combination 1), absence of both Zn^{2+} and Ca^{2+} ions (combination 2), absence of Ca^{2+} and
22 presence of Zn^{2+} ion (combination 3), absence of Zn^{2+} and presence of Ca^{2+} ion (combination 4)

1 with the protein). Each model was subjected to energy minimization using OPLS-2005 force
2 field (Optimized Potentials for Liquid Simulations). Progressively weaker restraints were applied
3 to the non-hydrogen atoms and refinement procedure was performed based on the
4 recommendation of Schrödinger LLC (Schrödinger, LLC, New York, NY, 2014). Because Glide
5 used the full OPLS- 2005 force field at an intermediate docking stage and claimed to be more
6 sensitive to geometric details than other docking tools. The thiol hydrogen atoms and the most
7 likely positions of hydroxyl, protonation states and tautomers of His residues, and Chi ‘flip’
8 assignments for Asn, Gln and His residues were selected using the protein assignment script
9 shipped by Schrödinger. The minimizations were performed until the average root mean square
10 deviation of the non-hydrogen atoms reached 0.3 Å.

11 **Ligand preparation**

12 The molecule *clerodane diterpenoid* was drawn in Maestro (Schrödinger, LLC, New
13 York, NY, USA) and assigned the structure using the LigPrip package from Schrödinger, LLC,
14 New York, NY, USA. This structure was converted to mae (Maestro, Schrödinger, LLC, New
15 York, NY, USA) format and optimized using OPLS 2005 force field with default setting.²²

16 **Active site predictions**

17 The SVMP modeled protein from our previous work²¹ was used in this study. The
18 calcium ion was present in the N- and C- terminal segments in the SVMP protein. The zinc
19 binding environments of the consensus has HEXXHXXGXXHD sequence, which contains three
20 zinc- binding histidines (His138, His142, and His148) and a glutamate. The active site of SVMP
21 (combinations 1-4) was predicted using the SiteMap in maestro (Maestro, version 9.8,
22 Schrödinger, LLC, New York, NY, 2014) with default parameters and. Further, the active site

1 was predicted using fpocket.⁴² The possible binding sites were identified for various physical
2 descriptors such as size, degree of exposure, degree of enclosure, tightness, hydrophilic,
3 hydrogen-bonding possibilities, hydrophobic, and linking site points were used for identifying
4 possible binding sites.

5 **Molecular docking studies**

6 The selected compound *clerodane diterpenoid* was docked into the binding site of all the
7 combinations (combinations 1-4) SVMP using Glide XP of Glide module.²³ The shape and
8 properties of the receptors were represented on a grid by several sets of fields that progressively
9 provided more accurate scoring to the ligand poses. To soften the potential for non-polar parts of
10 the receptor, we scaled van der Waal radii of receptor atoms by 1.00 with a partial atomic charge
11 of 0.25. The grid was generated (12 Å x 12 Å x 12 Å) by specifying residue as a grid centre. The
12 geometric or hydrogen bonding constraints were not introduced for substrate docking. Hydrogen
13 bonding and geometric constraint were not introduced in the substrate docking. Experiments
14 were performed using default parameters.

15 **Quantum polarized ligand docking (QPLD)**

16 The selected compound *clerodane diterpenoid* was docked with improved docking
17 program of quantum polarized ligand docking (QPLD).²²⁻²⁶ The QPLD was included with
18 quantum mechanical and molecular mechanical (QM/MM) calculations.^{27, 29} The QPLD docking
19 was carried out in three steps, the normal Glide docking with the best ligand poses acted as the
20 first step. In the second step, the charges were calculated from the QM calculations and the
21 partial charges were replaced on the ligand in the field of receptor for each ligand complex. The
22 single point electrostatic calculation was used with 6-31G*/LACVP* base set and B3LYP

1 density functional theory. The “Ultrafine” SCF accuracy level ($i_{\text{acc}} = 1$, $i_{\text{ac-scf}} = 2$) was used for the
2 QM region. In the final step, the ligand was redocked with updated atomic charges with the help
3 of Glide XP and QPLD and this step returned the most energetically favorable poses.

4 **Prime/MM-GBSA calculations**

5 The prime/MM-GBSA calculation based on the docking complex was used to calculate
6 the binding free energy (ΔG_{bind}) of the ligand. The docked poses were minimized by local
7 optimization feature in prime. The OPLS-AA 2005 force field was used for calculating binding
8 energy for a set of ligand and their receptor. The binding free energy was calculated by the
9 following equation.

$$10 \quad \Delta G_{\text{bind}} = \Delta E_{\text{MM}} + \Delta G_{\text{solv}} + \Delta G_{\text{SA}}$$

11 Here ΔE_{MM} is the difference in the minimized energies between the protein-ligand complexes.
12 ΔG_{solv} is the difference in the GBSA solvation energy of the protein-ligand complex and sum of
13 the solvation energies for the protein and ligand. ΔG_{SA} is the difference in the surface area
14 energies for the complex and sum of the surface area energies in the protein and ligand. The
15 minimizations of the docked complexes were performed with local optimization feature of
16 prime.

17 **QM-MM interaction energy calculation**

18 The QM-MM calculations were carried out with Glide XP docking of the *clerodane*
19 *diterpenoid* inhibitor and binding to the active site of SVMP for all the combinations (1-4).²⁶ The
20 QM-MM interaction energy was investigated using frozen orbital-based and hybrid QM-MM
21 potentials,^{30,31,41} which implemented in the Schrödinger Suite.²⁶ The hybrid potential combining

1 (i) density functional theory (DFT) with B3LYP functional to describe the atoms at the active
2 site of SVMP and (ii) include the molecular mechanics in the effect on protein matrix was used
3 for the protein ligand complex. Single point energy calculations and geometry optimized
4 structures were used with the basis set of LACVP** on the ligand.^{32,33} The geometry
5 optimization of the 6-31G** atoms and OPLS-2005 force field was used with rest of the
6 system.³⁴ The QM region of the all coordinates was free to adjust during the optimization.

7 **Molecular electrostatic potential (MESP) calculation**

8 The molecule *clerodane diterpenoid* from the docking study for all the combinations (1-
9 4) was used as an input for density functional theory (DFT) calculations. The DFT calculations
10 were performed using jaguar.²⁵ The complete geometry optimization was carried out by hybrid
11 density functional theory with Becke's three-parameter exchange potential and the Lee-Yang-
12 Parr correlation functional (B3LYP) and 6-31G** basis set level was used. The energy
13 calculations, simulate physiological conditions were performed by aqueous environment and
14 using Poisson-Boltzmann solver. Quantum chemical descriptors, MESP, HOMO, LUMO, and
15 salvation energy were carried out by Jaguar. The electrostatic potentials surface was created over
16 the ligand to provide a measure of the electrostatic potential at roughly the van der Waals surface
17 of the molecules. Further, the space was extending beyond the molecular surface which provided
18 a measure of charge distribution from the point of view an approaching reagent. The positive
19 electrostatic potential regions were indicated by excess positive charge. It was the repulsion of
20 positively charged test probe. The negative potential regions were indicated by the area of excess
21 negative charge. It was the attraction of positively charged test probe. 3D isosurfaces of the
22 MESP at the van der Waals contact surface represent electrostatic potentials superimposed onto
23 a surface of constant electron density (0.01eau^{-3}). The color coded isosurface values provide an

1 interaction of overall molecular size and location of positive or negative electrostatic potentials.
2 The deepest red and blue color was indicated by the most positive and the most negative
3 electrostatic potential regions.

4 **Molecular Dynamics Simulation**

5 The MD simulations of the protein ligand complexes for all the combinations (1-4) were
6 carried out using Desmond³⁵ and OPLS 2005 force field^{34,36} was used for energy minimization of
7 the system. The protein ligand complexes were solved in 10 Å×10 Å×10 Å cubic boxes with
8 periodic boundary conditions and TIP3 water molecules were solvated. The counter ions (Na⁺
9 and Cl⁻) were added in the whole system to balance the net charge. In Desmond, equilibration of
10 the whole system was carried out using default protocol made up of a series of restrained
11 minimizations and MD simulations. The minimized system was relaxed with NPT (number of
12 atom, pressure, and temperature) ensemble restraining non hydrogen solute atom for 50ns
13 simulation period. The Long range electrostatic interactions were computed by particle-mesh
14 Ewald method and van der waals (VDW) cut-off was set to 9 Å. The final confirmation of the
15 protein ligand complexes was performed by 50 nano seconds (ns) of MD simulations. The
16 structural changes and dynamic behavior of the protein were calculated by RMSD.

17 **Results and Discussion**

18 **Active prediction and molecular docking**

19 The active site of SVMP (combinations 1-4) was predicted using the SiteMap in maestro
20 (Maestro, version 9.8, Schrödinger, LLC, New York, NY, 2014) with default parameters.
21 Further, the active site of SVMP (combinations 1-4) was predicted using fpocket further this
22 binding cavity was compared to results predicted by SiteMap. Both the program was predicted

1 same binding site (supplementary figure 1). The molecular docking study was carried out by
2 Glide XP mode of docking (Schrödinger, LLC, New York, NY, 2014). The compound *clerodane*
3 *diterpenoid* was docked into the active site of SVMP. The protein-ligand interactions were
4 separated by four types like, hydrogen bonds, hydrophobic, ionic and water bridges. The amino
5 acids interactions were ZN1 (combination 1), HIS142, ILU166 (combination 2), ILU166,
6 ASP102 (combination 3) and HIS142 (combination 4). The catalytic zinc-ion is located at the
7 bottom of the active-site cleft. The zinc-binding environment is tetrahedral in this protein and
8 includes three histidines. The HIS142 is zinc binding residue in the SVMP protein. The histidine
9 (HIS142) functions as a ligand of the catalytic zinc atom in our protein. The calcium ion has
10 been identified opposite to the active site of SVMP and close to the cross-over point of N- and C-
11 terminal segments of M-domain (Calcium binding site). The M-domain is close to the calcium
12 binding site and opposing the catalytic zinc atom. This result clearly shows that HIS142,
13 LEU166 and ASP102 were important residues for ligand binding. In the presence of zinc ion, the
14 carbonyl group was interacted with the protein and in the absence of both ions in the protein; the
15 carbonyl group was not interacted with the protein. The combination 2 and combination 4 have
16 high binding affinities of the docking glide score (-29.79kcal/mol and 31.14kcal/mol). Both ions
17 were present in the protein the Glide scores were less binding affinity (Table 1). Based on the
18 docking study, both the ions (Zn^{2+} and Ca^{2+}) have a significant effect on the ligand binding site.

19 **Quantum polarized ligand docking**

20 It is now well recognized that the accuracy of electric charges plays a critical role in
21 protein-ligand docking. The QPLD docking method was used to improve the docking accuracy
22 and more accurate treatment for the electrostatic interactions. The quantum mechanical
23 calculations were derived from the ligand charges in the active site region of the protein. Among

1 these four environmental conditions, the combination 2 and combination 4 have high binding
2 affinities of the QPLD glide score (-5.092kcal/mol and -4.969kcal/mol). The presence of Zn²⁺ ion
3 with the protein, the QPLD glide scores were less binding affinity (-4.216 and -3.930). The
4 QPLD scores were also well correlated with the Glide XP docking results.

5 **Prime/MM-GBSA calculations**

6 The MM-GBSA was carried out to calculate the binding free energy of *clerodane*
7 *diterpenoid* against SVMP and to investigate the role of ions in the protein ligand binding. The
8 results from our energetic analysis of the complexes were shown in Table 2. The binding free
9 energy calculation of the complexes was obtained by XP docking and QPLD docking strategies.
10 Prime MM/GBSA (ΔG_{bind}) range was -48.16kcal/mol (combination 1), -44.75kcal/mol
11 (combination 2), -40.76kcal/mol (combination 3) and -43.35kcal/mol (combination 4). Presence of
12 both ions from the protein was observed, the ΔG_{bind} score (-48.169 kcal/mol) was increased. In
13 combination 2 and combination 4, the $\Delta G_{\text{bind covalent}}$ scores were increased. The combination 1
14 and combination 3, the $\Delta G_{\text{bind covalent}}$ scores were almost similar (Table 2). For the combination 1,
15 ΔG_{bind} , $\Delta G_{\text{BindCoulomb}}$, $\Delta G_{\text{BindLipo}}$ and $\Delta G_{\text{BindSolv}}$ were increased but $\Delta G_{\text{BindHbond}}$ (-0.05 kcal/mol) and
16 $\Delta G_{\text{Bind Covalent}}$ (3.55 kcal/mol) were decreased. Further the QPLD Prime MM/GBSA ΔG_{bind} scores
17 were -32.39kcal/mol for combination 1, -52.47kcal/mol for combination 2, -48.89kcal/mol for
18 combination 3 and -51.11kcal/mol for combination 4 (Table 2). This result clearly shows that both
19 ions are required for catalytic activity of protein.

20 **QM-MM interaction energy calculation**

21 **Molecular electrostatic potential (MESP) profiles**

1 Stereo electronic complementary of ligands and receptors are studied in detail by 3D
2 MESP and other electronic parameters since these properties are mainly driven the molecular
3 recognition in ligand-receptor interactions.^{37,38} The structural complementarities of the molecules
4 to the receptor were confirmed by docking analysis. Further, in order to understand the surface
5 electronic properties of the *clerodane diterpenoid*, we estimated the pharmacophoric features and
6 their complementary surface required for binding. Based on this idea, the molecule was analyzed
7 through MESP, HOMO-LUMO parameters and solvation energy (Table 3). The MESP
8 isosurface *clerodane diterpenoid* compound is superimposed inside the active site of SVMPP
9 (Figure 1A-D and Figure 2E-H). We mainly focused on the dihydrofuran-2(3H)-one side chain
10 which is adjacent to the Zn^{2+} ion. Obviously, the presence of both electropositive and
11 electronegative portions of *clerodane diterpenoid* makes this compound more reactive. Two
12 different portions namely dihydrofuran-2(3H)-one and 2,3dimethyl cyclohexanol are mainly
13 involved in the protein-ligand interaction with the key active site residues such as ASP102,
14 HIS142 and LEU166. As we mentioned earlier, the presence of zinc ion in the active site plays
15 an important role for ligand binding. The presence of most electronegative atoms in side chain
16 plays important role in making contact with the zinc atom. In the absence of zinc atom, the
17 oxygen atom of the group interacted with atom of LEU166. Thus the presence of electronegative
18 atom in *clerodane diterpenoid* is the structural requirement for the activity of this molecule.

19 **Highest occupied and lowest unoccupied molecular orbitals**

20 The orbital energies of HOMO and LUMO were also calculated and reported in Table 3.
21 In protein ligand binding, systematically, the electron acceptor ability of LUMO plays a vital role
22 when compare to electron donor property of HOMO. The HOMO eigenvalues for the *clerodane*
23 *diterpenoid* molecule is more negative, which indicates that higher HOMO energies and thus

1 stable binding of electrons to the nuclei. The more negative values of LUMO indicate lower
2 LUMO energy and strong affinity for electrons. The stability of the molecule is also confirmed
3 by calculated energy gap between HOMO and LUMO. HOMO-LUMO gap is an acute parameter
4 to determine the molecular admittance. Thus, the largest HLG value indicates a more stable
5 molecule and the rearrangement of its electron density.^{38,39} HOMO and LUMO maps were
6 visualized as π - like orbital for the possible molecular interaction analysis.⁴⁰ In the presence and
7 absence of ions the HOMO and LUMO sites are plotted onto the molecular surface of the
8 compound *clerodane diterpenoid* as shown in figure 3A-D (HOMO) and figure 4A-D (LUMO).
9 The reactive features and substituent influence on the electronic structure of the compounds were
10 characterized by these quantum chemical calculations results. Initially, we analyzed the HOMO
11 maps and we found that the HOMO maps had surrounded around 2,3 dimethyl cyclohexanol
12 group of the ligand. Docking results of these compounds also revealed the involvement of this
13 particular group in protein-ligand interactions. In case of LUMO, the LUMO maps were
14 surrounded in the dihydrofuran-2(3H)-one group of the compound. The results obtained from the
15 QM-MM study are quite reliable with the docking analysis and MESP results of the compounds
16 which demonstrate the participation of these moieties in the key protein-ligand interactions.

17 **Molecular dynamics simulation of protein ligand complexes**

18 The molecular dynamics (MD) simulation study was performed to check the stability and
19 dynamic prosperities of the protein-ligand complexes. The MD simulations were carried out by
20 four environmental conditions for the combinations 1-4. The dynamic stability of the complexes
21 was assessed during the MD simulation and RMSDs of the backbone was plotted in figure 5. The
22 combination 1 backbone RMSD of the protein was more stable in the simulation period of 50ns
23 when compare to combination 2 and combination 4. In combination 2, the RMSD of the protein

1 was fluctuated at 6Å from 10 to 17ns; it was increased abruptly to 6.5Å at 15ns and finally it was
2 stabilized after 40ns (Figure 5). For combination 3, the RMSD was fluctuated at 5Å from 1 to
3 20ns and it was stabilized after 20ns when compare to combination 2 and combination 4 (Figure
4 5). In combination 4, the RMSD protein was more fluctuated 3 to 20ns when compare to other
5 three RMSDs (Figure 5). This RMSD reached maximum deviation in 3 to 40ns; it could be
6 because of Zn²⁺ ion absence in the protein.

7 The RMSDs of the ligands in the active site of SVMP are shown in figure 6. Although
8 the RMSD of the combination 1 was more stable in the simulation period of 50ns when compare
9 to combination 3-4. For the combination 2, the RMSD of the ligand was significantly fluctuated
10 from 0 to 30ns. Hence, based on these RMSD analyses, the Zn²⁺ and Ca²⁺ ions are essential for
11 the stability and structure of the protein. The SVMP has maximum effect in the ligand binding in
12 the presence of Zn²⁺ ion when compared to Ca²⁺ ion. Binding pockets of Zn²⁺ and Ca²⁺ ions are
13 shown in the supporting files (Movie 1-4). Indicating the coordination of these metal ions leads
14 to conformational changes in the ligand binding. The metal ions are stabilizing the SVMP
15 protein.

16 Residue distance analysis

17 The residue distances were calculated to identify the temporal charges and location of the
18 residues. The distance matrix maps were displayed in the figure 7. In Combination 2, the color
19 coding region (blue color) of a helix was fluctuated more (figure 7B) whereas in combination 3,
20 the α helix regions (blue color) were also fluctuated during the simulation period of 20ns (figure
21 7C). In the presence of both Zn²⁺ and Ca²⁺ ions, it was not fluctuated much (figure 7A). Overall,

1 the above results show that the Zn^{2+} and Ca^{2+} ions were crucial for the interactions between the α -
2 helix and β sheet.

3 **Protein secondary Structure**

4 The protein secondary structure results were shown in the figure 8A-D. The
5 conformations of the alpha helixes were analyzed for four different conditions as explained in
6 previous chapters (Present and absence of ions Zn^{2+} and Ca^{2+}). Alpha helical conformations were
7 more conserved in the simulation period of 50ns. Loss of small amount alpha helix was observed
8 at 0 to 50ns of the secondary structure of protein (figure 8B, 8D) in absence of Zn^{2+} ion of all the
9 combinations. Similar observations were also noticed in the β strand region for both Zn^{2+} and
10 Ca^{2+} ion combinations. This was reflected in MD simulation graphs at 50ns particularly in the
11 residue region of 150-170 (Figure 8). The Zn^{2+} and Ca^{2+} ions play a vital role in structural stability
12 of the α helix and β strand regions of protein.

13 **Protein-Ligand Contacts**

14 The MD simulation trajectory analysis was carried out to refine and understand the
15 binding nature of protein-ligand complexes. In the combination 1, complex of SVMP, the
16 molecule *clerodane diterpenoid* had high consistent ionic bond network with HIS138, GLU139,
17 HIS142 and HIS 148 up to 50ns. Interestingly, this compound had capability in formation of
18 ionic mediated bridges with zinc atom (Figure 9A).

19 In combination 2, nine intermolecular hydrogen bonds were observed. The residues were
20 HIS148, GLN152, ASN154, CYS155, GLY156, ALA157, CYS160, THR167 and GLN169
21 (Figure 9B). The number of interactions was increased because of absence of Zn^{2+} ion at the
22 complex.

1 Whereas in combination 3, it exhibited 10 H-bonds and the interactive amino acid
2 residues were THR103, ILE104, GLY105, HIS138, GLU139, HIS148, GLN152, SER163,
3 ALA164 and LEU166. At 50ns of MD simulation, the hydrogen bond interaction of the residues
4 HIS138, GLU139 and HIS148 had more stability.

5 Combination 4 has 9 H bonds (THR103, HIS138, GLU139, HIS148, CYS160, VAL161,
6 SER163, THR165 and THR167) in throughout MD simulation. The number of interactions were
7 increased due to the absence of Zn^{2+} ion at the complex (Figure 9D).

8 **The importance of ions**

9 The docking, QPLD, binding free energy calculation and MD simulation results shows
10 that Zn^{2+} ion in the active site of SVMP has a critical function. Since we could not find any
11 significant changes in the Glide score, Glide energy and binding free energy for the different
12 SVMP models were calculated. The binding free energy was reduced vigorously in the absence
13 of Zn^{2+} and Ca^{2+} ions; whereas, it was not deviated in the presence of Ca^{2+} and Zn^{2+} ions. The
14 amino acids of 5 to 196 were calcium binding region and 138 to 149 were zinc binding region.
15 The His138, GLU139, His142, and His148 were important active site of the protein and that
16 function as ligands of the catalytic zinc atom. In MD simulation result shows that, the His138,
17 GLU139, His142, and His148 were ionic bond interactions (Combination 1). In absence of ion
18 (Zn^{2+} or Ca^{2+}) with the protein, these residues were interacted only hydrogen bond interactions. In
19 absence of both ions with the protein, these restudies were no interactions. Based on these
20 results, the metal ions are stabilizing the SVMP protein and critically required for the catalytic
21 activity of SVMP protein.

22

1 Conclusion

2 The role of Zn²⁺ and Ca²⁺ ions in the protein (SVMP) were analysed. The compound
3 *clerodane diterpenoid* was analysed by molecular docking, quantum polarized ligand docking
4 and the active site of SVMP by QM-MM methods. The molecular dynamics simulations were
5 performed up to 50ns using Desmond to understand the role of ligand in the active site of SVMP
6 protein by various combinations (combinations 1-4). In the absence of both Zn²⁺ and Ca²⁺ ions
7 from the protein, MD simulation RMSDs were fluctuates, particularly absence of Zn²⁺ ion with
8 the protein, the RMSDs were more fluctuates (5000 to 12500 ps). Based on the results, we
9 conclude that the Zn²⁺ and Ca²⁺ ions have a vital role in the active site of SVMP protein.

10 Acknowledgements

11 The authors gratefully acknowledge the infrastructure facilities provided by the
12 Department of Bioinformatics, Alagappa University, Post Graduate Diploma in Structural
13 Pharmacogenomics (funded by UGC, Government of India. No. F.14-13/2013 (Inno/ASIST)
14 dated 30.03.3013).

15 References

- 16 1. R. M. Kini and H. J. Evans, *Toxicon*, 1992, **30**, 265-293.
- 17 2. O. H. Ramos and H. S. Selistre-de-Araujo, *Comp Biochem Physiol C Toxicol Pharmacol*,
18 2006, **142**, 328-346.
- 19 3. T. Sajevic, A. Leonardi and I. Krizaj, *Toxicon*, **57**, 627-645.
- 20 4. S. D. Aird, *Toxicon*, 2002, **40**, 335-393.
- 21 5. J. W. Fox and S. M. Serrano, *J Proteomics*, 2009, **72**, 200-209.

- 1 6. K. F. Huang, S. H. Chiou, T. P. Ko and A. H. Wang, *Eur J Biochem*, 2002, **269**, 3047-
2 3056.
- 3 7. M. M. Mendes, S. A. Vieira, M. S. Gomes, V. F. Paula, T. M. Alcantara, M. I. Homs-
4 Brandeburgo, J. I. dos Santos, A. J. Magro, M. R. Fontes and V. M. Rodrigues,
5 *Phytochemistry*, **86**, 72-82.
- 6 8. J. M. Gutierrez, A. Rucavado, T. Escalante and C. Diaz, *Toxicon*, 2005, **45**, 997-1011.
- 7 9. F. S. Markland, *Toxicon*, 1998, **36**, 1749-1800.
- 8 10. R. M. Kini, *Toxicon*, 2005, **45**, 1133-1145.
- 9 11. T. Escalante, N. Ortiz, A. Rucavado, E. F. Sanchez, M. Richardson, J. W. Fox and J. M.
10 Gutierrez, *PLoS One*, **6**, e28017.
- 11 12. S. Takeda, H. Takeya and S. Iwanaga, *Biochim Biophys Acta*, **1824**, 164-176.
- 12 13. J. B. Bjarnason and J. W. Fox, *Pharmacol Ther*, 1994, **62**, 325-372.
- 13 14. J. M. Gutierrez, A. Rucavado, T. Escalante and C. Diaz, *Toxicon*, 2005, **45**, 997-1011.
- 14 15. A. Rucavado, J. Nunez and J. M. Gutierrez, *Int J Exp Pathol*, 1998, **79**, 245-254.
- 15 16. A. S. Kamiguti, F. P. Rugman, R. D. Theakston, F. O. Franca, H. Ishii and C. R. Hay,
16 *Thromb Haemost*, 1992, **67**, 484-488.
- 17 17. T. Escalante, J. Nunez, A. M. Moura da Silva, A. Rucavado, R. D. Theakston and J. M.
18 Gutierrez, *Toxicol Appl Pharmacol*, 2003, **193**, 17-28.
- 19 18. S. E. Gasanov, R. K. Dagda and E. D. Rael, *J Clin Toxicol*, **4**, 1000181.
- 20 19. S. M. Han, F. A. Weaver, A. J. Comerota, B. A. Perler and M. Joing, *J Vasc Surg*, **51**,
21 600-609.

- 1 20. E. N. Baramova, J. D. Shannon, J. B. Bjarnason and J. W. Fox, *Arch Biochem Biophys*,
2 1989, **275**, 63-71.
- 3 21. S. Chinnasamy, S. Chinnasamy, S. Nagamani and K. Muthusamy, *J Biomol Struct Dyn*,
4 1-12.
- 5 22. LigPrep, version 3.1, Schrödinger, LLC, New York, NY, 2014.
- 6 23. Glide, version 6.4, Schrödinger, LLC, New York, NY, 2014.
- 7 24. Schrödinger Suite 2014-3 QM-Polarized Ligand Docking protocol
- 8 25. Jaguar version 8.5, Schrödinger, LLC, New York, NY, 2014.
- 9 26. QSite version 6.4, Schrödinger, LLC, New York, NY, 2014.
- 10 27. A. E. Cho, V. Guallar, B. J. Berne and R. Friesner, *J Comput Chem*, 2005, **26**, 915-931.
- 11 28. P. Kirubakaran, P. Arunkumar, K. Premkumar and K. Muthusamy, *Mol Biosyst*, **10**,
12 2699-2712.
- 13 29. K. D. Singh and K. Muthusamy, *Acta Pharmacol Sin*, **34**, 1592-1606.
- 14 30. M. Dean, Philipp, A. Richard and Friesne, *J Comput Chem*, 1999, **20**, 1468-94.
- 15 31. R. B. Murphy, D. M. Philipp, R. A. Friesner, *J Comput Chem*, 2000, **21**, 1442-57.
- 16 32. S. K. Tripathi and S. K. Singh, *Mol Biosyst*, **10**, 2189-2201.
- 17 33. P. J. Hay and W. R. Wadt, *J. Chem. Phys.*, 1985, **82**, 299–310.
- 18 34. W. L. Jorgensen, D. S. Maxwell, and J. Tirado-Rives, *Am. Chem. Soc.* 1996, **45**, 11225-
19 11236.
- 20 35. J. Kevin Bowers, Edmond Chow, Huafeng Xu, O. Ron Dror, P. Michael Eastwood, A.
21 Brent Gregersen, L. John Klepeis, István Kolossváry, A. Mark Moraes, D. Federico
22 Sacerdoti, K. John Salmon, Yibing Shan, and E. David Shaw, 2006 *Proceedings of the*
23 *ACM/IEEE Conference on Supercomputing (SC06)*, Tampa, Florida, November 11–17.

- 1 36. A. George, Kaminski, A. Richard, Friesner, Julian Tirado-Rives, L. William and
2 Jorgensen, *J Phys Chem B*, 2001, **105**, 6474-87.
- 3 37. A. K. Bhattacharjee and J. M. Karle, *Bioorg. Med. Chem.*, 1998, **6**, 1927-1933.
- 4 38. R. U. Kadam, D. Garg, A. T. Paul, K. K. Bhutani and N. Roy, *J. Med. Chem.*, 2007, **50**,
5 6337-6342.
- 6 39. R. G. Parr and R. G. Pearson, *J. Am. Chem. Soc.*, 1983, **105**, 7512–7516.
- 7 40. H. Cao, X. Pan, C. Li, C. Zhou, F. Deng and T. Li, *Bioorg Med Chem Lett*, 2003, **13**,
8 1869-1871.
- 9 41. J. C. Phillips, R. Braun, W. Wang, J. Gumbart, E. Tajkhorshid, E. Villa, C. Chipot, R. D.
10 Skeel, L. Kale and K. Schulten, *J Comput Chem*, 2005, **26**, 1781-1802.
- 11 42. Peter Schmidtke, Vincent Le Guilloux, Julien Maupetit, Pierre Tuffery, *Nucleic Acids*
12 *Research*, 2010, 1–8 doi:10.1093/nar/gkq383.

13
14
15
16
17
18
19
20
21
22
23
24

1 **Tables**

2 **Table 1:** Combinations 1-4 analyzed by docking simulations studies and their corresponding
 3 Glide scores, Glide energy and hydrogen bond interactions.

S. No	Ions	Glide XP docking			QPLD docking		
		Glide score (kcal/mol)	Glide energy (kcal/mol)	H-bond interactions	Glide score (kcal/mol)	Glide energy (kcal/mol)	H-bond interactions
1	Combination 1	-2.66	-27.56	ZN1	-4.21	-37.22	ZN1, VAL109
2	Combination 2	-4.27	-29.79	HIS142, ILU166	-5.09	-34.98	HIS142, ILU166
3	Combination 3	-3.44	-25.53	ILU166, ASP102	-3.93	-29.15	ILU166, ASP102
4	Combination 4	-4.18	-31.14	HIS142	-4.96	-37.79	HIS142, ILU166

4
 5 **Combination 1:** Presence of both Zn²⁺ and Ca²⁺ ions; **Combination 2:** Absence of both Zn²⁺
 6 and Ca²⁺ ions; **Combination 3:** Absence of Ca²⁺ and Presence of Zn²⁺ ion; **Combination 4:**
 7 Absence of Zn²⁺ and Presence of Ca²⁺ ion.

8 **Table 2:** Binding free energy results for the combinations 1-4.

S. No	Ions	Binding free energy(kcl/mol) (Docking)							Binding free energy(kcl/mol) (QPLD)						
		ΔG Bind	ΔG Bind Coulomb	ΔG Bind Covalent	ΔG Bind Hbond	ΔG Bind Lipo	ΔG Bind SolvGB	ΔG Bind vdW	ΔG Bind	ΔG Bind Coulomb	ΔG Bind Covalent	ΔG Bind Hbond	ΔG Bind Lipo	ΔG Bind SolvGB	ΔG Bind vdW
1	Combination 1	-48.16	-14.15	3.55	-0.05	-36.61	29.31	-30.21	-32.39	-20.51	0.21	-0.24	-17.77	27.90	-21.98
2	Combination 2	-44.75	-17.58	5.77	-0.41	-30.42	24.28	-26.39	-52.47	-17.81	4.14	-0.42	-30.16	22.73	-30.95
3	Combination 3	-40.76	-3.73	3.08	-0.52	-24.42	9.66	-24.82	-48.89	-21.01	6.87	-0.47	-31.14	20.34	-23.49
4	Combination 4	-43.35	-11.93	6.52	-0.18	-29.86	23.25	-31.14	-51.11	-16.78	4.18	-0.42	-30.03	21.67	-29.73

9
 10 **Combination 1:** Presence of both Zn²⁺ and Ca²⁺ ions; **Combination 2:** Absence of both Zn²⁺
 11 and Ca²⁺ ions; **Combination 3:** Absence of Ca²⁺ and Presence of Zn²⁺ ion; **Combination 4:**
 12 Absence of Zn²⁺ and Presence of Ca²⁺ ion.

13

14

15

1 **Table 3:** QM-MM energy, HOMO, LUMO, HELG and MESP parameter of the combinations 1-4.

S. No	Ions	QM-MM energy (kcal mol ⁻¹)	HOMO (eV)	LUMO (eV)	HLG (eV)	MESP (kcal mol ⁻¹)	
						Most positive potential	Most negative potential
1	Combination 1	-1212.89	0.05	0.14	0.09	60.66	-92.70
2	Combination 2	-1208.60	0.16	0.38	0.22	54.20	-53.42
3	Combination 3	-1208.78	0.06	0.27	0.21	69.40	-43.13
4	Combination 4	-1207.94	0.12	0.34	0.22	49.24	-53.35

2
 3 **Combination 1:** Presence of both Zn²⁺ and Ca²⁺ ions; **Combination 2:** Absence of both Zn²⁺
 4 and Ca²⁺ ions; **Combination 3:** Absence of Ca²⁺ and Presence of Zn²⁺ ion; **Combination 4:**
 5 Absence of Zn²⁺ and Presence of Ca²⁺ ion.

6 7 **Figures**

8 Figure 1. MESP superimposed onto a surface of constant electron density for combination 1 and
 9 combination 2. Showing the most positive potential region (deepest blue color) and most
 10 negative potential regions (deepest red color) in the active site of SVMP.

11 Figure 2. MESP superimposed onto a surface of constant electron density for combination 3 and
 12 combination 4. Showing the most positive potential region (deepest blue color) and most
 13 negative potential regions (deepest red color) in the active site of SVMP.

14 Figure 3. Plots of the highest occupied molecular orbital of combinations 1-4.

15 Figure 4. Plots of the lowest unoccupied molecular orbital of combinations 1-4.

16 Figure 5. The backbone RMSD of the protein the whole simulation time.

17 Figure 6. The RMSD of the *clerodane diterpenoid* in the active site of SVMP.

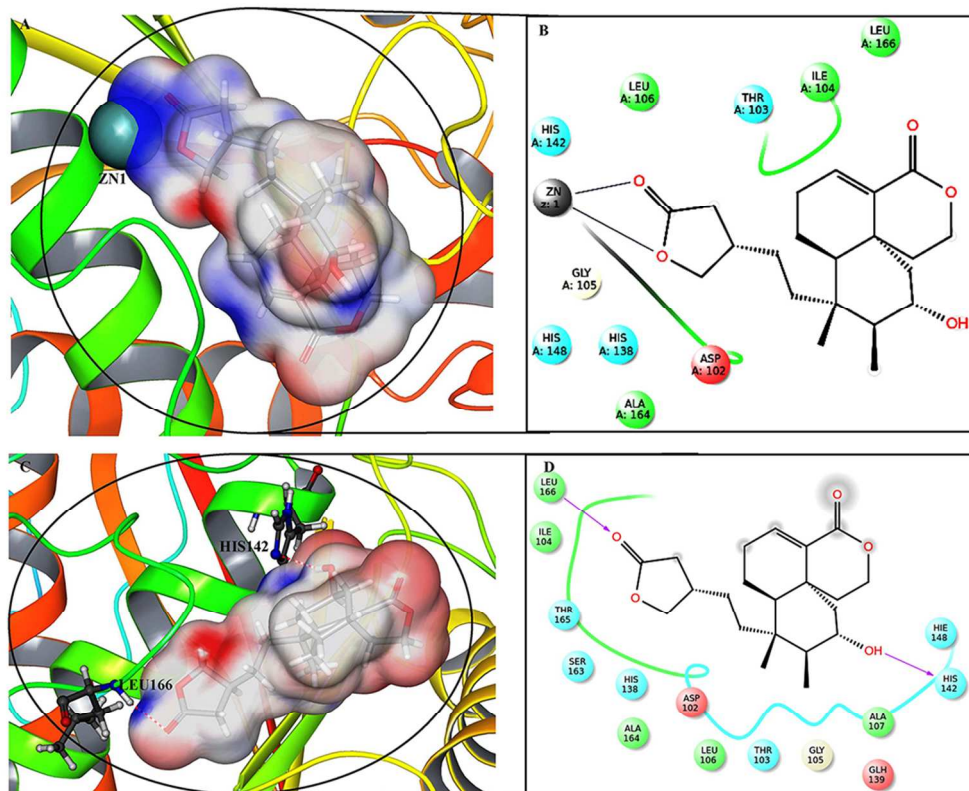
18 Figure 7. Matrices of the smallest distances between residue pairs for combinations 1-4.

19 Figure 8. The evaluation of the secondary structure of combinations 1-4.

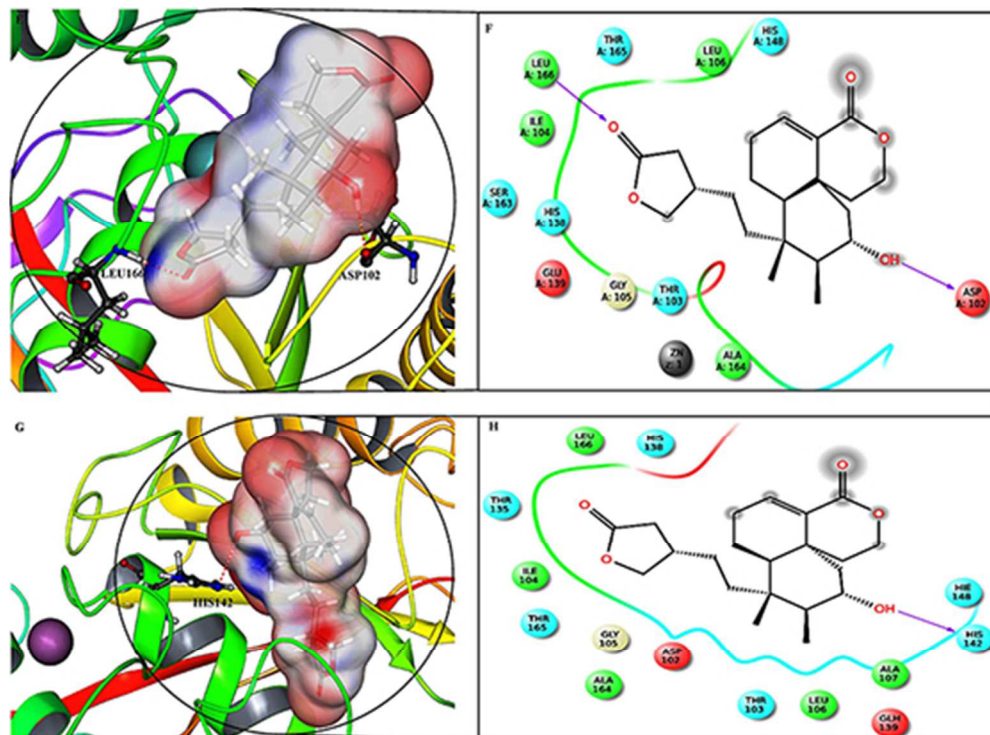
20 Figure 9. Protein-ligand contacts through 50ns simulation (combinations 1-4).

1 Supporting files

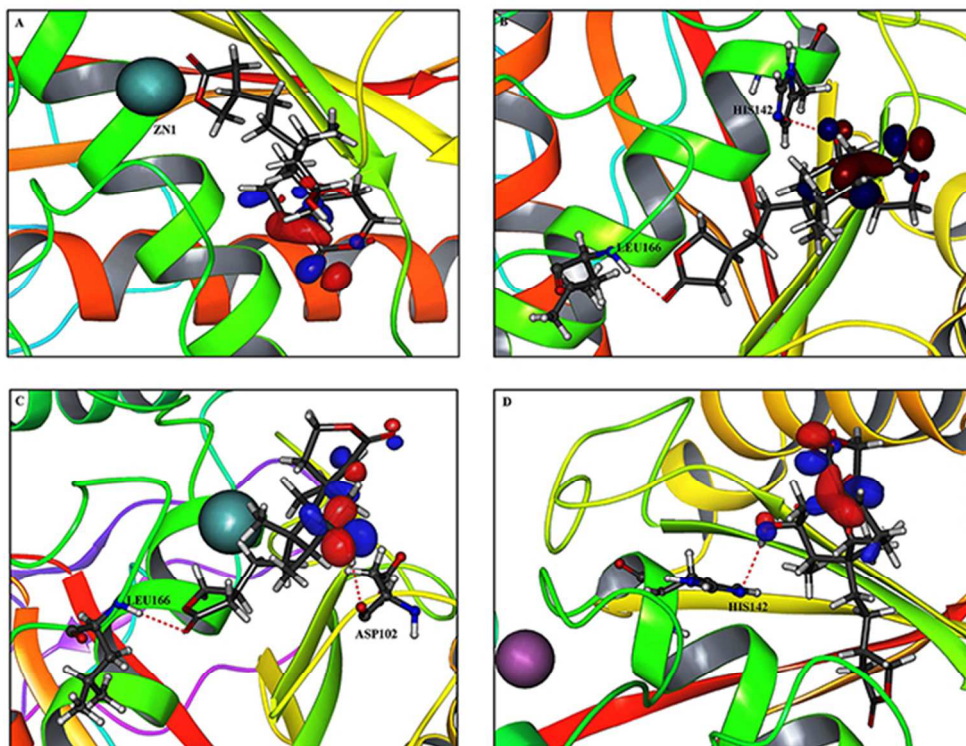
- 2 Supplementary Figure 1. Binding cavity of SVMP (Combinations 1-4) using SiteMap and
- 3 Fpocket (Combination 1 A, B. Combination 2 C, D. Combination 3 E, F and Combination 4 G,
- 4 H).
- 5 Movie 1-4. The binding pockets of the Zn^{2+} and Ca^{2+} ions from the SVMP protein.



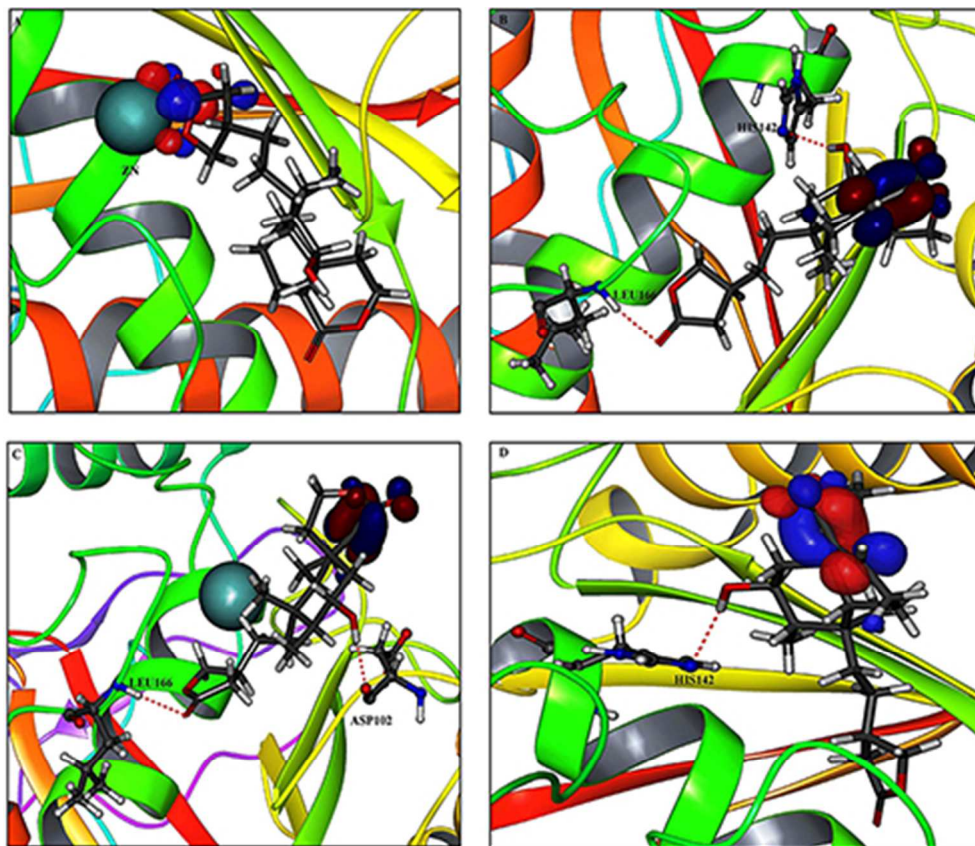
MESP superimposed onto a surface of constant electron density for combination 1 and combination 2. Showing the most positive potential region (deepest blue color) and most negative potential regions (deepest red color) in the active site of SVMP
126x102mm (224 x 224 DPI)



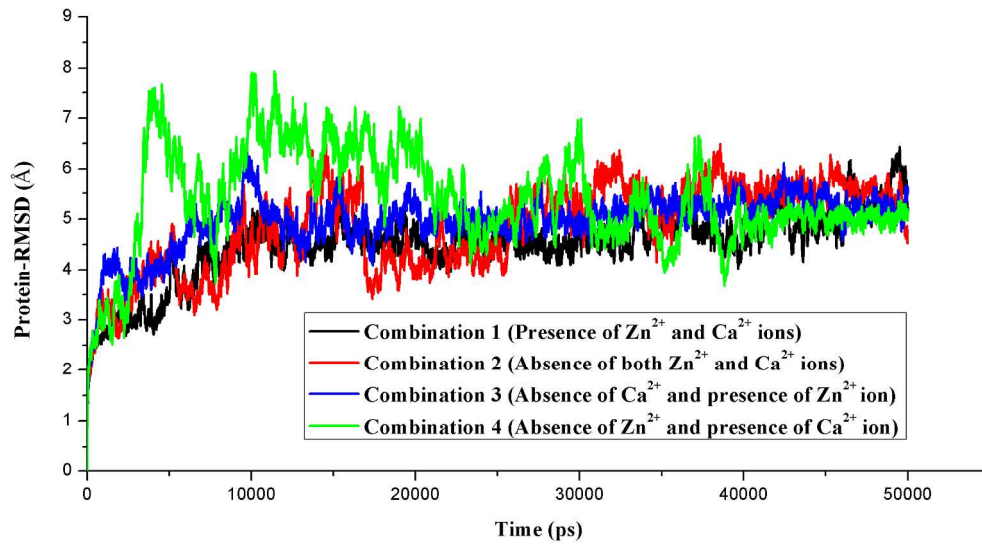
MESP superimposed onto a surface of constant electron density for combination 3 and combination 4. Showing the most positive potential region (deepest blue color) and most negative potential regions (deepest red color) in the active site of SVMP.
70x53mm (202 x 202 DPI)



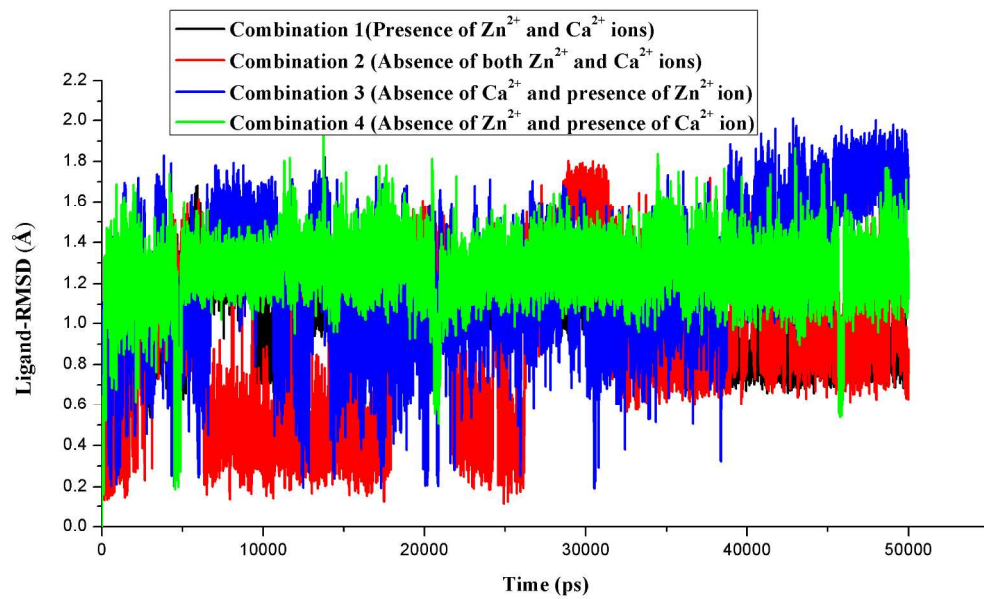
Plots of the highest occupied molecular orbital of combinations 1-4.
77x60mm (218 x 218 DPI)



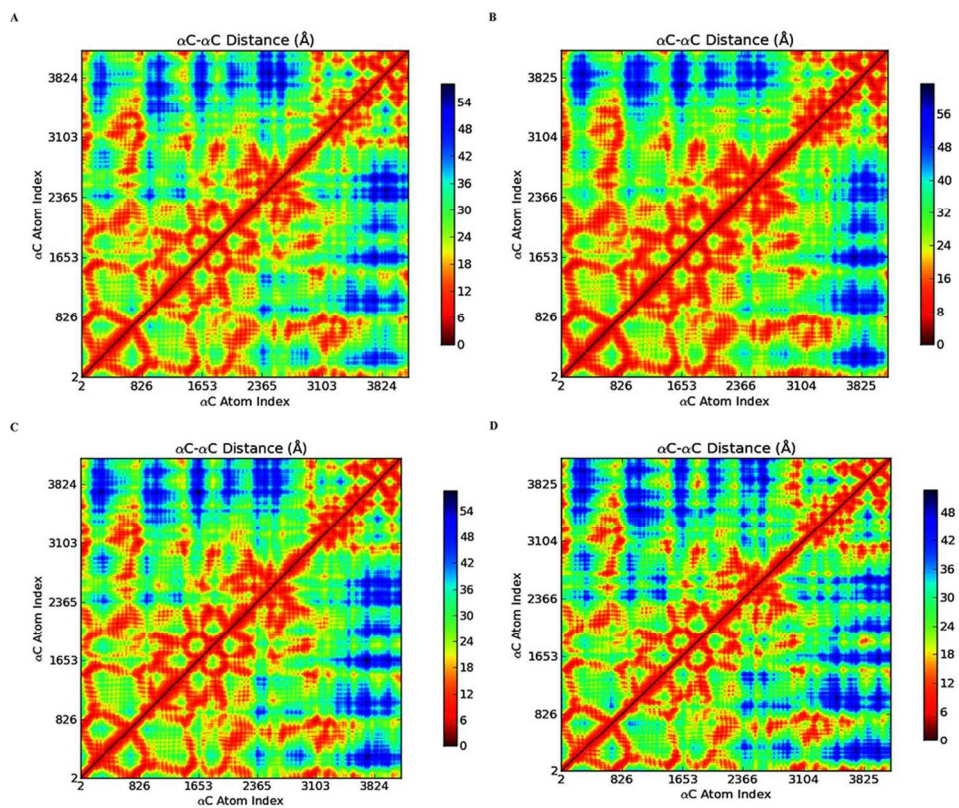
Plots of the lowest unoccupied molecular orbital of combinations 1-4.
72x62mm (173 x 173 DPI)



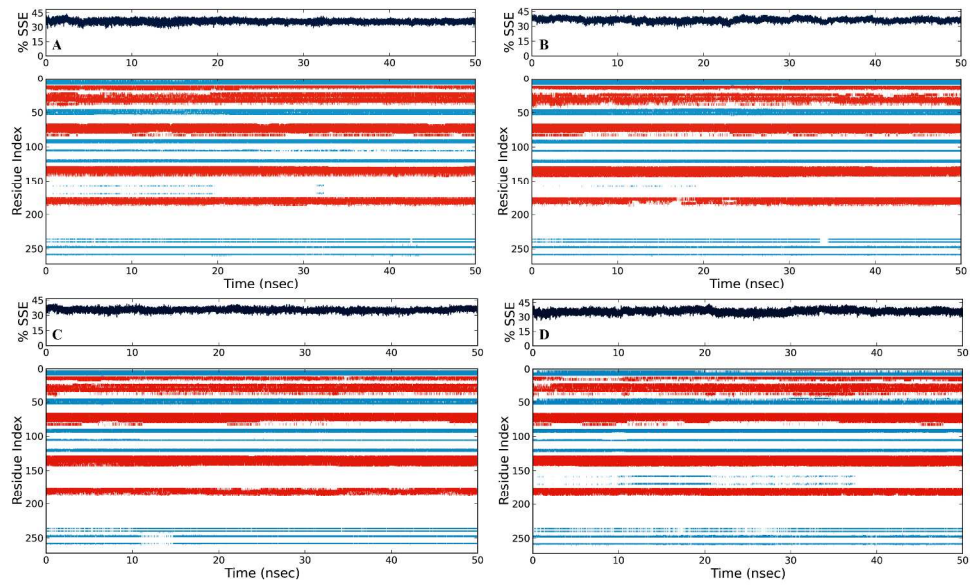
The backbone RMSD of the protein the whole simulation time.
205x114mm (300 x 300 DPI)



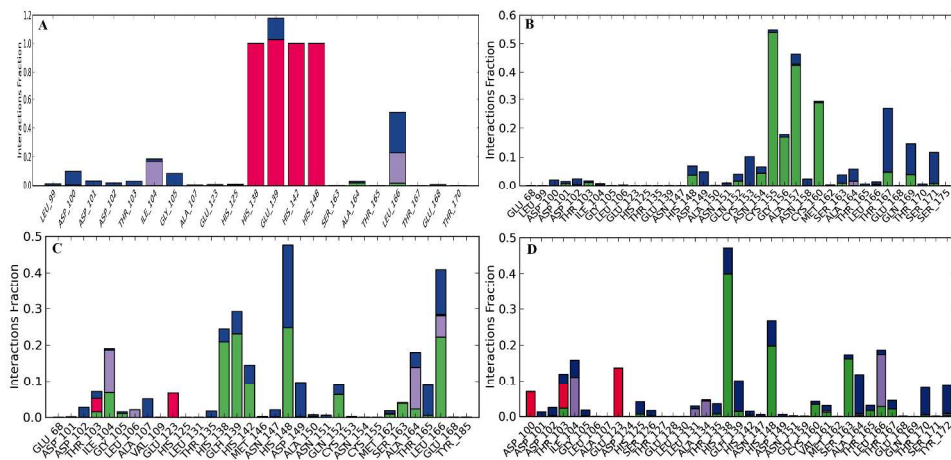
The RMSD of the clerodane diterpenoid in the active site of SVMP.
209x124mm (300 x 300 DPI)



Matrices of the smallest distances between residue pairs for combinations 1-4.
138x117mm (200 x 200 DPI)



The evaluation of the secondary structure of combinations 1-4.
489x305mm (220 x 220 DPI)



Protein-ligand contacts through 50 ns simulation (Combinations 1-4).
503x247mm (220 x 220 DPI)